

Article

Enhancing System Reliability and Transient Voltage Stability through Optimized Power Sources and Network Planning

Fan Li ¹, Dong Liu ¹, Dan Wang ¹, Wei Wang ^{2,*}, Zhongjian Liu ¹, Haoyang Yu ¹, Xiaofan Su ^{3,4}, De Zhang ^{3,4} and Xiaoman Wu ²

¹ State Grid Economic and Technological Research Institute Co., Ltd., Beijing 102209, China; fllewis@163.com (F.L.)

² Department of Electrical Engineering, Xi'an Jiaotong University, Xi'an 710049, China

³ Hunan Key Laboratory of Energy Internet Supply-Demand and Operation, Changsha 410082, China

⁴ State Grid Hunan Electric Power Company Limited Economic & Technical Research Institute, Changsha 410029, China

* Correspondence: wangwei1223@stu.xjtu.edu.cn; Tel.: +86-180-6729-6193

Abstract: Renewable energy is an important means of addressing climate change and achieving carbon peaking and carbon neutrality goals. However, the uncertainty and randomness of renewable energy also have a certain impact on the flexibility, reliability, and transient voltage stability of the power system. These effects also pose great challenges to power system planning. In order to address the impact of renewable energy on power system planning, this paper proposes a two-layer optimization model for power sources and network planning which takes into account both reliability and transient voltage stability requirements. The upper-layer grid planning problem is formulated with consideration of the system reliability index, and the transient stability requirements and construction and operation costs are included in the lower-layer problem to determine a construction scheme for power generation and energy storage units. To solve the complex nonlinear problem efficiently, a two-layer iterative algorithm utilizing the adaptive particle swarm optimization (PSO) technique is proposed. The effectiveness of the proposed method is demonstrated via its application to the IEEE 33 test system. The results show that the proposed optimization approach effectively addresses the power system transmission and generation planning problem while improving the efficiency and reliability of the system's operation. The findings can guide the design and implementation of future power system planning and operation strategies.

Keywords: generation and transmission planning; reliability; transient voltage stability



Citation: Li, F.; Liu, D.; Wang, D.; Wang, W.; Liu, Z.; Yu, H.; Su, X.; Zhang, D.; Wu, X. Enhancing System Reliability and Transient Voltage Stability through Optimized Power Sources and Network Planning. *Electronics* **2023**, *12*, 3190. <https://doi.org/10.3390/electronics12143190>

Academic Editors: Jožef Ritonja, Le Zheng and Mohammed Agamy

Received: 8 June 2023

Revised: 5 July 2023

Accepted: 5 July 2023

Published: 23 July 2023



Copyright: © 2023 by the authors. Licensee MDPI, Basel, Switzerland. This article is an open access article distributed under the terms and conditions of the Creative Commons Attribution (CC BY) license (<https://creativecommons.org/licenses/by/4.0/>).

1. Introduction

Climate change is a major and urgent global challenge facing all of humanity [1]. Against the background of the emission peak and carbon neutrality targets set by the Chinese government, the power industry must shoulder the responsibility of reducing greenhouse gas emissions [2]. Developing clean energy, increasing the proportion of electricity in primary energy consumption, and improving the level of electrification on the energy consumption side are important ways to achieve the goal of carbon neutrality by 2060 [3]. To this end, the capacity of renewable energy in power systems is growing rapidly. The new power system, which is dominated by wind power, photovoltaic power, and other forms of renewable energy, tends to replace the traditional high-carbon power system that is based on fossil fuels. Nonetheless, the uncertainty and strong variability of renewable energy will lead to a sharp contradiction with the need to ensure a continuous and stable power supply [4], posing challenges for the planning and operation of power systems [5,6].

In order to increase the flexibility of the power system, a significant amount of research has been conducted on the integrated planning of power sources and networks, with the aim of achieving an optimized and coordinated solution [7–9]. In [10], a coordinated

expansion planning method for renewable energy and transmission lines was proposed, demonstrating the economic advantages of coordinated expansion. In [11], a multi-objective optimization model for the generation expansion problem that included transmission constraints was applied to reach trade-offs between cost and environmental impacts. In [12], a static planning method was formulated. To better cope with the challenges brought by the uncertainty of renewable energy, stochastic optimization and robust optimization were adopted in relevant research studies. A stochastic adaptive robust optimization approach to system planning was proposed in [13]. In [14], a stochastic multistage co-planning model of transmission expansion and battery energy storage systems (BESSs) was proposed. A robust optimization method for transmission network planning was proposed in [15] which specified the uncertainty of net injection as a simple uncertainty set instead of the probability distribution. In [5], a comprehensive robust planning model was formulated that considered the power ramping requirements and construction periods accompanying the increasing integration of renewable generation.

Reliability is a crucial requirement in power system planning under the influence of a high degree of penetration of renewable energy as it guarantees safe and economical operation. Many works have investigated probabilistic planning models considering the reliability criteria of power systems [16–18]. The expansion planning model considering the reliability objective was proposed in [16] and was able to achieve a more economical and reliable result. The cost of expected energy not supplied (EENS) was considered in the optimization objective to determine the construction scheme of generator set and circuit. A stochastic co-optimization planning model that considers long-term probabilistic reliability, specifically, the loss of load expectation (LOLE), was proposed in [17]. In [18], a method was provided for choosing the best transmission plan while considering the reliability indices.

Further, in terms of system transient voltage stability, the time domain simulation method [19], direct method [20], and artificial intelligence method [21] have been applied for analysis in existing research. The direct method analyzes the transient stability of the system quantitatively by constructing a transient energy function [22,23]. In addition, the influence of the scale and layout of renewable energy access on the system's transient voltage stability can be simulated via the time domain simulation method [24]. However, due to the lack of rigorous theoretical derivation support, it is difficult to evaluate the transient stability of power systems quantitatively using the above-mentioned methods. To study the characteristics of a dynamic response under external disturbances and to quantify the external disturbances that the power system can withstand, the input-to-state stability (ISS) theory can be applied [25,26].

The generation and transmission planning problem of power systems is essentially a multi-dimensional optimization problem with complex constraints [27]. Mathematical optimization algorithms and heuristic algorithms are generally used to solve planning problems. In [11], a multi-objective method based on mixed integer linear programming was proposed. A heuristic algorithm was proposed in [12] to optimize the economic plan while reinforcing the reliability level. To solve this problem, the heuristic method can deal with discrete variables well and has global convergence in theory at present. The particle swarm optimization (PSO) algorithm has high search efficiency, fast convergence speed, and simple operation. Therefore, it has attracted the attention of many scholars at home and abroad since it was proposed. In [28], a multi-objective PSO algorithm with adaptive weight was proposed. The inertia weight and learning factor were adjusted. To perform mutation operations on particles outside of stable conditions, a stable mutation operator was proposed in [29]. The hybrid method enhances the local exploration ability of particles. In [30], a modified particle swarm optimization with dynamic momentum was proposed based on SPO. A multi-level optimization method based on PSO was provided to solve a three-object operating problem in [31].

In summary, a significant amount of research has been performed on power generation and transmission system planning with a high proportion of renewable energy access. However, a planning method that considers both the adequacy of system regulation

capacity and transient voltage stability must still be further investigated. In this paper, a planning method for a transmission and generation system that integrates reliability and transient voltage stability is proposed. A two-layer model of transmission and generation planning is established. Considering the cost of construction, the reliability criterion EENS, and the transient stability index, a multi-objective function is constructed. Based on the optimization of network construction in the upper layer, the sites, capacities and the operation cost of energy resources are optimized in the lower layer while restricting the influence of renewable energy on the system stability. A heuristic-based iterative algorithm is applied to solve the two-layer optimization problem. The results show that the comprehensive optimization objective of system planning is improved.

The rest of this paper is organized as follows: in Section 2, the mathematical formulation of the two-layer generation and transmission planning problem is formulated. The solution method is proposed in Section 3. Case studies are presented in Section 4 to demonstrate the effectiveness of the proposed method. The conclusion of this article is provided in Section 5.

2. Mathematical Formulation

A two-layer planning model has been established for power system design and optimization. The upper layer of the model focuses on optimizing the transmission planning scheme to ensure the economy and reliability of the system. In the lower layer, the model seeks to optimize the capacity and location of traditional generators, renewable energy sources, and energy storage units based on the optimized transmission plan from the upper layer. This two-layer model aims to strike a balance between system cost-effectiveness, reliability, and transient stability in power system design and operation. By optimizing both the transmission planning and power generation and storage allocation, the two-layer planning model can lead to a more reliable and sustainable power system.

2.1. Grid Planning

2.1.1. Objective Function

To ensure the economy and reliability of the planning results, the construction cost of the transmission lines and the system reliability are comprehensively considered in the objective.

$$\min F_1 = C_{inv} + C_r \tag{1}$$

where C_{inv} denotes the cost of network investment, and the cost of the EENS is represented by C_r . The formulation can be written as follows:

$$C_{inv} = \sum_{t \in \Omega^T} \sum_{l \in \Omega^{L+}} \kappa_t x_{lt} L_l C_l^{inv} \tag{2}$$

$$\kappa_t = \frac{1}{(1+r)^{t-1}} \tag{3}$$

where κ_t denotes the coefficient of the present-worth value. r is the discount rate. x_{lt} is a binary variable that is equal to 1 if line l is built and 0 otherwise, representing the investment state of line l in time t . L_l represents the length of the line l . C_l^{inv} represents the investment cost of the transmission line l per unit length.

The reliability optimization objective is expressed as the cost of the EENS, which can be written as follows:

$$C_r = \gamma \times \sum_{t \in \Omega^T} \sum_z \sum_j P_z \Gamma_{zjt} dt \tag{4}$$

where γ is the cost coefficient of the lost load [32]. P_z denotes the probability of contingency z . Γ_{zjt} denotes the load shedding of the electric load j in time t (MW). dt is the time duration of interval t .

2.1.2. Constraints

1. Constraints of the construction scheme:

Decision variables of the construction scheme shall meet the requirements as follows.

$$x_{l(t-1)} \leq x_{lt} \quad \forall l \in \Omega^{L+} \tag{5}$$

where $x_{lt} \in \{0, 1\}$ represents the investment state of line l . Ω^{L+} indicates the set of lines to be built.

2. Capacity constraints of transmission lines:

To comply with the upper limit requirement, it is imperative to ensure that the transmission lines possess adequate capacity.

$$S_l \leq S_{\max} \tag{6}$$

where S_l is the construction capacity of line l . S_{\max} denotes the upper limit of transmission capacity permitted.

3. Network connectivity and open-loop operation constraints:

Power systems are required to deliver electric power to all load points while avoiding the creation of an annular power supply structure. The restrictions are expressed as follows:

$$\sum_{e \in \Omega_{LL} \cap \Omega_{EL}} x_e + \sum_{k \in \Omega_{LL} \cap \Omega_{NL}} x_k \leq N_{LL} - 1 \quad \forall \Omega_{LL} \tag{7}$$

where Ω_{LL} , Ω_{EL} , Ω_{NL} are the set of branches contained in the annular structure, existing lines, and prospective lines, respectively. N_{LL} denotes the total number of branches in the set Ω_{LL} . x_e, x_k are the construction states of lines e and k , respectively.

2.2. Power Generation and Energy Storage Planning

2.2.1. Objective Function

In the lower layer of the model, the construction and operational costs associated with conventional generating units, new energy units, and energy storage units, as well as the transient voltage stability index, are considered in the optimization objective. A comprehensive objective function is formulated to achieve the optimal allocation of resources for power generation and energy storage.

$$\min F_2 = C_{dinv} + C_{oper} + \lambda \cdot \rho \tag{8}$$

$$C_{dinv} = \sum_{t \in \Omega^T} \sum_{g \in \Omega^{G+}} \kappa_t (x_{gt} - x_{g(t-1)}) P_g C_g^{inv} + \sum_{t \in \Omega^T} \sum_{w \in \Omega^{W+}} \kappa_t (x_{wt} - x_{w(t-1)}) P_w C_w^{inv} + \sum_{t \in \Omega^T} \sum_{p \in \Omega^{P+}} \kappa_t (x_{pt} - x_{p(t-1)}) P_p C_p^{inv} + \sum_{t \in \Omega^T} \sum_{s \in \Omega^{S+}} \kappa_t (x_{st} - x_{s(t-1)}) E_s C_s^{inv} \tag{9}$$

$$C_{oper} = \sum_{t \in \Omega^T} \kappa_t F_{3t} \tag{10}$$

where C_{dinv} denotes the construction costs of conventional generators, new energy units, and energy storage. $C_g^{inv}, C_w^{inv}, C_p^{inv}, C_s^{inv}$ refer to the investment costs per unit capacity of conventional units, wind turbine units, photovoltaic units, and energy storage systems, respectively. P_g, P_w, P_p are the rated capacities of conventional generators, wind turbine generators, and photovoltaic units, respectively. E_s is the rated capacity of the energy storage system. C_{oper} denotes the operation costs during the studied period. F_{3t} is the optimal daily operation cost, which is solved via operational optimization.

According to the input-to-state stability theory, the transient voltage stability of a power system is related to the grid structure, as well as the installed capacities of con-

ventional and new energy generation units. The spectral radius of the small-gain matrix, which is denoted by ρ , is used to quantify the transient voltage stability of the system. A smaller value of ρ corresponds to a higher level of transient stability for power systems. It is incorporated into the objective function in the form of a weighted sum, with the weighting coefficient λ representing the importance of the transient stability index.

2.2.2. Constraints

1. Constraints of the construction scheme:

The variables of the construction scheme should satisfy the following constraints:

$$\begin{aligned} x_{g(t-1)} &\leq x_{gt} \quad \forall g \in \Omega^{G+} \\ x_{w(t-1)} &\leq x_{wt} \quad \forall re \in \Omega^{W+} \\ x_{p(t-1)} &\leq x_{pt} \quad \forall re \in \Omega^{P+} \\ x_{s(t-1)} &\leq x_{st} \quad \forall s \in \Omega^{S+} \end{aligned} \tag{11}$$

where $x_{gt}, x_{wt}, x_{pt}, x_{st} \in \{0, 1\}$ represent the construction states of a generator g , wind turbine generator w , photovoltaic units p , and energy storage s , respectively. $\Omega^{G+}, \Omega^{RE+}, \Omega^{S+}$ are sets of components to be built.

2. Output constraints of generators:

$$P_{g,\min} \leq P_g \leq P_{g,\max} \quad \forall g, \forall t \tag{12}$$

where $P_{g,\max}, P_{g,\min}$ are the maximum and minimum allowable construction capacities of generator i , respectively, and are determined based on the given transmission planning scheme.

3. Capacity constraints of new energy units:

$$\begin{aligned} P_{w,\min} &\leq P_w \leq P_{w,\max} \\ P_{p,\min} &\leq P_p \leq P_{p,\max} \end{aligned} \tag{13}$$

where $P_{w,\max}, P_{w,\min}$ are the upper and lower limits of the capacity of wind farm w , respectively. $P_{p,\max}, P_{p,\min}$ are the capacity limits of photovoltaic units p , respectively.

4. Capacity constraints of the energy storage system:

$$E_{s,\min} \leq E_s \leq E_{s,\max} \tag{14}$$

where $E_{s,\max}, E_{s,\min}$ denotes the maximum and minimum capacity of the energy storage device s .

5. Power balance constraint:

$$\sum_{i \in \Psi_n^G} g_{it} + \sum_{w \in \Psi_n^W} p_{wt} + \sum_{p \in \Psi_n^P} p_{pt} - \sum_{s \in \Psi_n^S} p_{st} - \sum_{l: s(l)=n} f_{lt} + \sum_{l: r(l)=n} f_{lt} = \sum_{j \in \Psi_n^D} d_{jt} \quad \forall n, \forall t \tag{15}$$

where g_{it}, p_{wt}, p_{pt} denote the generated output of a conventional generator i , wind turbine generator w , and photovoltaic unit p at time t , respectively. p_{st} denotes the power exchanged between energy storage s and the system at time t , which is negative when the energy storage is discharged. f_{lt} represents the active power flow of line l connected to node n . $r(l), s(l)$ denote the starting and ending nodes of line l , respectively. d_{jt} is the load demand. $\Psi_n^G, \Psi_n^W, \Psi_n^P, \Psi_n^S, \Psi_n^D$ are the set of generators, wind turbines, photovoltaic power stations, energy storage, and loads at node n , respectively.

6. Power flow constraint:

The existing transmission lines must satisfy the following power flow constraint equations:

$$\begin{cases} -f_l^{\max} \leq f_{lt} \leq f_l^{\max} & l \in \Omega^{L_0}, \forall t \\ f_{lt} - \frac{(\theta_{st} - \theta_{rt})}{X_l} = 0 & l \in \Omega^{L_0}, \forall t \end{cases} \quad (16)$$

For the expanded transmission lines, the constraints are as follows:

$$\begin{cases} -x_{lt}f_l^{\max} \leq f_{lt} \leq x_{lt}f_l^{\max} & \forall t \\ -(1 - x_l)M \leq f_{lt} - \frac{(\theta_{st} - \theta_{rt})}{X_l} \leq (1 - x_l)M & \forall t \end{cases} \quad (17)$$

where X_l represents the line reactance. f_l^{\max} denotes the line capacity. θ_{st}, θ_{rt} are the phase angles of the voltage at the starting and ending nodes of line l , respectively. Ω^{L_0} is the set of existing lines.

7. Phase angle constraints of node voltage:

The phase angle of the node voltage must remain within the specified limits, which can be written as follows:

$$\begin{cases} -\pi \leq \theta_{st} \leq \pi \\ -\pi \leq \theta_{rt} \leq \pi \end{cases} \quad (18)$$

8. Proportion constraint on the installed capacity of new energy:

The proportion of the newly installed capacity of renewable energy to the overall newly installed capacity of the system in that year should not be less than the required proportion, which is expressed as follows:

$$\sum_{i \in \Omega^{RE}} x_{it} P_i^{\text{rated}} \geq \rho_t \cdot \sum_{i \in \Omega^{RE} \cup \Omega^G} x_{it} P_i^{\text{rated}}, \forall t \quad (19)$$

where ρ_t is the sequence of the installed capacity proportion of the new energy sources. By changing the value of ρ_t , the proportion of new energy sources in the system can be adjusted. P_i^{rated} denotes the rate capacity of power sources i .

9. Transient stability constraint:

According to the input-to-state stability (ISS) theory [33], the system must satisfy the stability constraint as follows to ensure the transient voltage stability level of the system.

$$\rho(G^{IOS}) < 1 \quad (20)$$

$$G^{IOS} = \Gamma^{IOS} Z \quad (21)$$

where G^{IOS} denotes the small-gain matrix. $\rho(G^{IOS})$ is the spectral radius of the small-gain matrix G^{IOS} . Z is the input–output connection matrix determined by the network structure. Γ^{IOS} denotes the input–output gain matrix determined by the installed capacities of the new energy sources and conventional units at the node and is formulated as follows:

$$\Gamma^{IOS} = \begin{bmatrix} \gamma_1^{IOS} & 0 & \dots & 0 \\ 0 & \gamma_2^{IOS} & \dots & 0 \\ \vdots & \vdots & \ddots & \vdots \\ 0 & 0 & \dots & \gamma_n^{IOS} \end{bmatrix} \quad (22)$$

where $\gamma_1^{IOS}, \gamma_2^{IOS}, \dots, \gamma_n^{IOS}$ denote the input–output gains of subsystems 1, 2, ..., n , correspondingly.

2.3. Operation Strategy

Based on the system structure obtained via the two-layer model, the optimal operation model of the lower layer is formulated. The objective function is to minimize the overall operating cost of the system, which is expressed as follows:

$$\min F_3 = C_{gen} + C_{ess} \tag{23}$$

We have

$$\begin{aligned} C_{gen} &= \sum_{t \in \Omega^T} \sum_{i \in \Omega^G} \kappa_t g_{it} du_t G_i \\ C_{ess} &= \sum_{t \in \Omega^T} \sum_{s \in \Omega^S} \zeta p_{st} du_t \end{aligned} \tag{24}$$

where C_{gen} denotes the operation cost of conventional generators. G_i denotes the coefficient of operation cost (\$/MWh). du_t is the duration of time period t . g_{it} denotes the output of unit i . C_{ess} represents the operation cost of energy storage. p_{st} denotes the power exchanged between the energy storage device s and the system. ζ is the coefficient of C_{ess} .

The operational constraints are given as follows:

$$\sum_{i \in \Psi_n^G} g_{it} + \sum_{r \in \Psi_n^{RE}} (P_r \cdot p_{rt}^* - p_{rdt}) - \sum_{s \in \Psi_n^S} p_{st} - \sum_{l:s(l)=n} f_{lt} + \sum_{l:r(l)=n} f_{lt} = \sum_{j \in \Psi_n^D} d_{jt} \quad \forall n, \forall t \tag{25}$$

$$x_{gt} g_{it}^{\min} \leq g_{it} \leq x_{gt} g_{it}^{\max} \quad \forall i, \forall t \tag{26}$$

$$\Delta r_g^{\min} \leq g_{it} - g_{it-1} \leq \Delta r_g^{\max} \quad \forall i, \forall t \tag{27}$$

$$-p_{s,max} \leq p_{st} \leq p_{s,max} \tag{28}$$

$$0 \leq e_{st} \leq E_s, \quad \forall s, t \tag{29}$$

$$e_{s0} = e_{sN} \tag{30}$$

$$e_{st} = e_{st-1} + \alpha_s p_{st} du_{t-1} \tag{31}$$

$$\alpha_s = \begin{cases} \eta_{cs} & p_{st} > 0 \\ \frac{1}{\eta_{ds}} & p_{st} \leq 0 \end{cases} \tag{32}$$

$$\begin{cases} p_{w,\min} \leq p_{wt} \leq p_{w,\max} \\ p_{p,\min} \leq p_{pt} \leq p_{p,\max} \end{cases} \quad \forall p, w \in \Omega^{RE+}, \forall t \tag{33}$$

$$\begin{cases} \sum_{i \in \Psi_n^G} g_{it}^{\max} + \sum_{r \in \Psi_n^{RE}} (P_r \cdot p_{rt}^* - p_{rdt}) \geq \sum_{j \in \Psi_n^D} d_{jt} + R_t^{up} \\ \sum_{i \in \Psi_n^G} g_{it}^{\min} + \sum_{r \in \Psi_n^{RE}} (P_r \cdot p_{rt}^* - p_{rdt}) \leq \sum_{j \in \Psi_n^D} d_{jt} - R_t^{dn} \end{cases} \quad \forall n, \forall t \tag{34}$$

Constraint (25) enforces the power balance at each bus, where the variable of wind and solar power curtailment p_{rdt} is introduced. Since the DC power flow model is adopted in network modeling, the wasting of circuitry is not considered. P_r is the rated capacity of the new energy unit r at node n , and p_{rt}^* is the normalized value of its generated output at time t . Constraints (26) and (27) restrict the operation of conventional generators, which include thermal power units and gas turbines. Constraint (26) regulates the output power range of generator i at time t . The maximum and minimum generation power, $g_{it}^{\max}, g_{it}^{\min}$, are decision variables which are related to the operating state and ramping capability of the unit. Given the high proportion of new energy sources being integrated, the equivalent

net load variation of the system has intensified. Conventional units should be capable of providing sufficient ramping capacity to compensate for power imbalances in the system. The ramping constraints of the generating units are formulated in Constraint (27), in which $\Delta r_g^{\max}, \Delta r_g^{\min}$ denote the ramp-up and ramp-down capabilities per unit of time.

Constraints (28)–(32) formulate the operational constraints of energy storage. As given in (28), the charging and discharging power of energy storage is limited within the rated power $p_{s,\max}$. p_{st} denotes the power exchanged between the energy storage unit s and the system, satisfying $p_{st} > 0$ when the energy storage device is charged and $p_{st} < 0$ in the discharging state. In (29), the stored energy in the device should be limited within the rated capacity range E_s during operation. e_{st} is the remaining energy of energy storage unit s at time t . Moreover, in (30), to ensure the circulatory regulation capability of the energy storage system during its operation, the stored energy at the end of the operating cycle should be restored to the same level as the initial energy level. e_{s0}, e_{sN} are the initial and final energy levels in the studied period, respectively. Constraints (31) and (32) represent the sequential coupling between the stored energy and the charge–discharge power of the energy storage system during operation. α_s denotes the efficiency coefficient of the charging and discharging of energy storage s . η_{cs} is the charging efficiency, while η_{ds} is the discharging efficiency.

Constraint (33) enforces the outputs of wind farms and photovoltaic power stations, in which $p_{w,\max}, p_{w,\min}$ denote the upper and lower limits of the active power of a wind farm w . Similarly, $p_{p,\max}, p_{p,\min}$ denote the limits of solar power. Additionally, in order to ensure a safe, reliable, and continuous supply of electricity, the power system is required to have a certain amount of reserve capacity in case of uncertainties such as the failure of new energy units and deviations from the predicted output. Therefore, the reserve capacity constraints are formulated in (34), in which R_t^{up}, R_t^{dn} denote the demand for reserve capacity in the positive and negative directions in the time period t .

3. Solution Method

The model presented in Section 2 comprises two layers involving grid planning, power generation and energy storage planning. The optimization problem, with its nonlinear complex constraints, is non-convex and poses a formidable challenge to conventional optimization methods in obtaining an effective solution. In view of this, a two-layer iterative algorithm utilizing the adaptive PSO technique is proposed for optimal planning scheme design.

3.1. Weight-Adaptive PSO Algorithm

In the current research, heuristic algorithms are often employed for solving optimal planning problems. Among them, the PSO algorithm is commonly used in system planning [34]. This paper also takes reliability into consideration [35].

The PSO algorithm is based on the principle of simulating the collective behavior of animals. It utilizes the genetic and selection mechanisms found in nature to perform iterations, achieving fast convergence and high precision, making it suitable for solving nonlinear optimization problems. Prior to the initiation of the algorithm, a set of solutions represented by a set of points in the solution space is randomly initialized. During each iteration, the point set is updated using the best positions found by the swarm and each point. The optimal solution can be obtained after the iterations have been completed.

Specifically, the dimension of the solution space is set as N . Firstly, particle positions z and velocities v are randomly initialized. z corresponds to the decision variables in the optimization model, while v represents the planning configuration changes. After obtaining an initialized configuration that satisfies all the constraints, the position of the j th particle z_j is regarded as its currently searched optimal position $q_j (j = 1, 2, \dots, m)$, and the best position among the swarm is selected as the global optimal position g . Then, the iteration

process is carried out. In each iteration, the positions and velocities of the particles are updated with randomness, following the functions below.

$$\begin{aligned}
 v_j &\leftarrow Wv_j + C_1R_1(q_j - z_j) + C_2R_2(g - z_j) \\
 z_j &\leftarrow z_j + v_j
 \end{aligned}
 \tag{35}$$

where R_1, R_2 are random numbers uniformly distributed within the interval $[0,1]$. v_j is the velocity of the j th particle. W denotes the inertia weight. C_1, C_2 are the acceleration constants.

A larger value of the inertia weight W is advantageous in jumping out of local optima during the search, while a smaller W is conducive to algorithm convergence and improving search accuracy. An appropriate value of W can reach a trade-off between search accuracy and speed. In this study, an adaptive adjustment strategy for the inertia weight W is adopted. At the beginning of the iteration, a larger initial value of 0.9 was set, and it decreased linearly to 0.4 during the iterations.

Upon obtaining the updated positions and velocities of the particles, the algorithm evaluates whether the new solution satisfies the imposed constraints and exhibits improved objective function value. Only when both criteria are satisfied is the solution updated in the swarm. Otherwise, it remains unchanged. Following the update of all particles, the best position in the swarm is selected as the new global optimal position g . After the iteration, the global best position g of the swarm denotes the optimal solution derived by the algorithm.

3.2. Solution Process

A schematic diagram of the generation and transmission planning model is presented in Figure 1. The planning optimization is the primal problem, and the corresponding sub-problem, namely, the operating optimization, is solved based on candidate solutions for the planning scheme, with the operational solution feedback to the main problem. In the two-level planning problem, an iterative interaction between the transmission planning and source-storage planning schemes is performed, resulting in an overall optimal solution that satisfies both levels. Moreover, the objective functions and decision variables in the model are provided in the diagram.

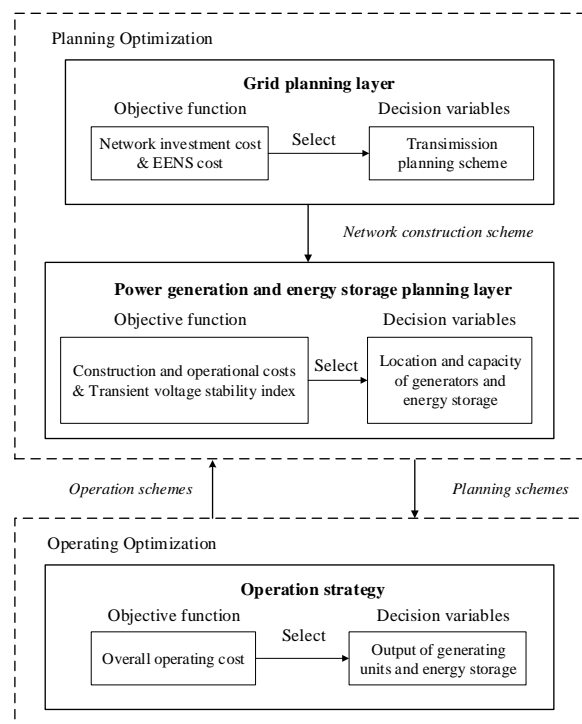


Figure 1. Schematic diagram of the generation and transmission planning.

Accordingly, by applying the improved weight-adaptive PSO algorithm, the two-layer generation and transmission planning model is solved. The overall solution process is as follows.

1. Solution procedure for grid planning:

Initialize the parameters of the particle population and generate N grid planning schemes in population X .

With the comprehensive aim of optimizing the line construction cost and system reliability, a subset of excellent individuals from the particle population X are selected for crossover and mutation to create N updated grid planning schemes.

Transfer N grid construction schemes to the lower-level encoding as input conditions for power supply, energy storage planning, and operational problem solving.

Calculate the fitness of particle population X and evaluate whether the iterative termination condition is reached. If the condition is met, the search ends, and the solution corresponding to the optimal individual is outputted. Otherwise, the population is updated, and the process returns to step 2.

2. Solution procedure for power generation and energy storage planning:

Generate a particle population Y for the access location and investment capacity of conventional units, new energy units, and energy storage based on the particle population X of the grid construction scheme obtained from the upper layer.

Considering the uncertainty of the generated output of new energy units, apply the Monte Carlo method to a sample wind speed and solar radiation intensity in each time period, and use a fuzzy C -means clustering algorithm to cluster the sampled new energy output scenarios, obtaining multiple typical scenarios.

Optimize the operation strategy for each generation unit and energy storage in investment schemes based on the generated output of the new energy units and scenario probabilities in typical scenarios. Then, calculate the system operating cost according to the scheduling scheme of conventional units and wind/solar power.

Calculate the fitness of particle population Y based on the comprehensive optimization objective, which is composed of the system operating cost, the energy generation and storage investment cost, and the transient voltage stability index corresponding to the planning scheme. Judge whether the iterative termination condition is reached, and execute step 4 if yes; otherwise, update the population and return to step 1.

Step 5: Return the main objective function value to the upper layer. Update the optimal value of the objective function and determine the optimal planning scheme accordingly.

4. Case Study

Utilizing the IEEE-33 standard as a basis, two distinct scenarios are established to validate the efficacy of the method through a comparative analysis. In Scenario 1, the generation planning scheme undergoes optimization exclusively. To distinguish these two scenarios, the grid structure is not optimized, and only the power generation and energy storage planning is carried out in Scenario 1. Conversely, Scenario 2 involves the implementation of the proposed planning model in Figure 1, which means that both the grid planning layer and power generation and energy storage planning layer are considered in Scenario 2.

4.1. Optimization Parameters

The optimization parameters are listed in Table 1. The values of all the upper and lower limits of constraints, like energy storage power, are listed as follows. Based on the multi-stage heuristic algorithm proposed in Section 3, the construction and operational costs of generation planning can be derived. The discount rate r is 5%. The value of the cost coefficient of lost load γ is set at 10,000 CNY/MWh. The population size and generations of the PSO algorithm are set to 100 each.

Table 1. System operating boundary conditions.

Optimization Parameter	Value (kW)
Maximum discharge power of energy storage	250
Maximum charging power of energy storage	−200
Maximum power of thermal power unit	250
Minimum power of thermal power unit	100
Maximum power of gas turbine	3000
Minimum power of gas turbine	100

4.2. Results of Optimization Objects

The optimal results are presented in Table 2. The cost of generation planning in two different scenarios can be seen as follows.

Table 2. Costs of generation planning in different optimization scenarios.

Scenario	Energy Storage Cost (CNY)	Thermal Power Unit Cost (CNY)	PV Cost (CNY)	Wind Turbine Cost (CNY)	Gas Turbine Cost (CNY)	Total Cost (CNY)
Scenario 1	3587	4309	1335	2908	6815	52,274
Scenario 2	3221	2842	1335	2908	7246	51,030

Table 2 depicts a performance comparison between the optimal schemes of Scenario 1 and Scenario 2, demonstrating that the latter yields superior economic benefits. Moreover, the value of the transient voltage stability index ρ is equal to 0.52 in Scenario 1, while in Scenario 2, the index achieves a smaller value of 0.15 through the generation and transmission planning method proposed in this paper. This outcome indicates a significant enhancement in the transient voltage stability of the system.

4.3. Comparison of Planning Results in Two Scenarios

The corresponding transmission planning results for two scenarios are presented in Figure 2. In the graph, the dashed line corresponds to the prospectively planned extension lines of Scenario 2.

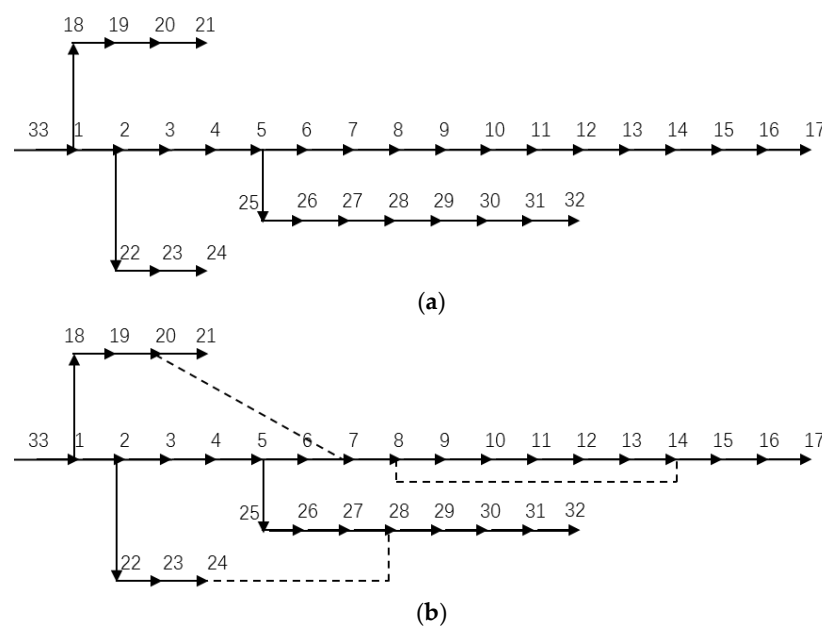


Figure 2. Transmission planning results. (a) System structure of Scenario 1; (b) optimal grid planning scheme of Scenario 2.

Additionally, Table 3 displays the locations of both generators and energy storage units in the two aforementioned scenarios.

Table 3. Access locations of generators and energy storage units in different optimization scenarios.

Scenario	Energy Storage	Gas Turbine	Thermal Power Unit	PV	Wind Turbine
Scenario 1	(12, 17)	(2, 21)	(26, 9)	(14, 6)	(24, 20)
Scenario 2	(12, 32)	(3, 24)	(28, 9)	(20, 7)	(29, 16)

In Scenario 1, the energy storage units are located at node 12 and node 17, the gas turbines are located at node 2 and node 21, the thermal power units are located at node 26 and node 9, the PV units are located at node 14 and node 6, and the wind turbines are located at node 24 and node 20. In scenario 2, implementing the proposed planning model in Figure 1, the energy storage units are located at node 12 and node 32, the gas turbines are located at node 3 and node 24, the thermal power units are located at node 28 and node 9, the PV units are located at node 20 and node 7, the wind turbines are located at node 29 and node 16.

4.4. Optimal Operation Results

Further, the optimal operation results under Scenario 2 are solved and analyzed. The figure below illustrates the operating schemes of the generators and energy storage units in the optimal planning scheme of Scenario 2.

In Figure 3, the abscissa in the diagram is the time axis, corresponding to each moment of 24 h in a day. The ordinate represents the power value, and the unit is kW. As shown in Figure 3a, photovoltaic power reaches a high level during the day, while wind power experiences a peak at night. The outputs of new energy resources are effectively utilized to meet the power demand. Additionally, energy storage units are also optimized to contribute to the power supply, as depicted in Figure 3b. Two power curves depict the outputs of the energy storage devices that connected to node 12 and node 32, respectively. According to the operating parameters, the energy and power curves meet the constraints. Meanwhile, Figure 3c,d display the outputs of thermal power units and gas turbines, respectively, which are also adjusted to fit the power supply in the optimal planning scheme. The results indicate that the proposed planning model is effective in integrating various power sources and storage units to optimize the power supply and meet the demand in the system.

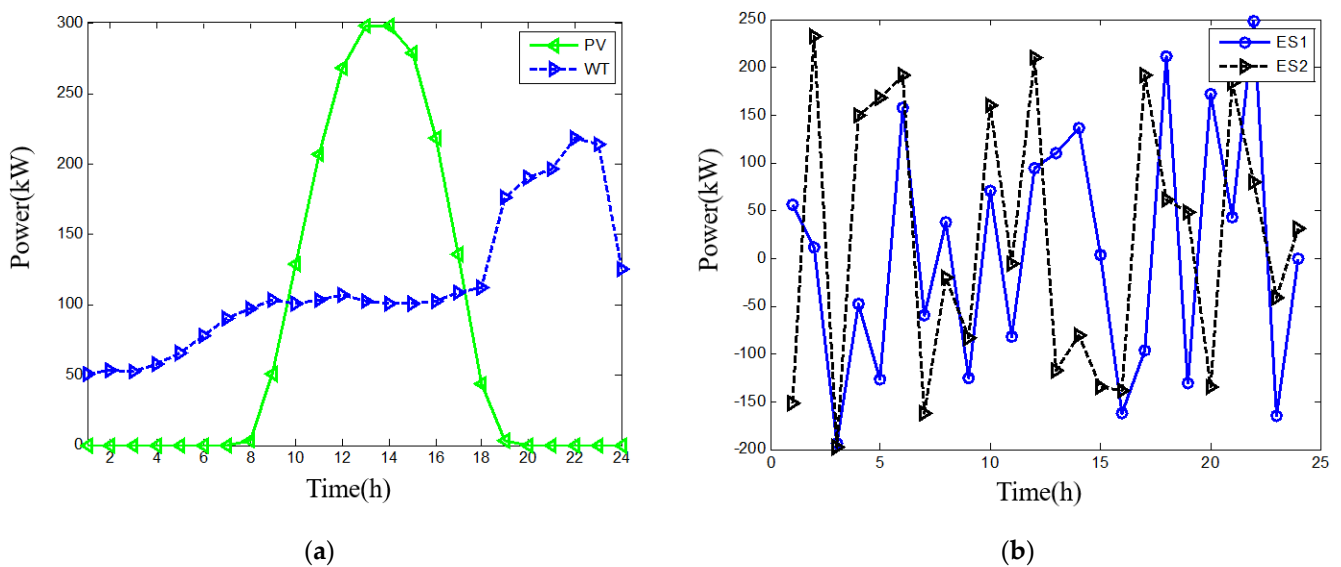


Figure 3. Cont.

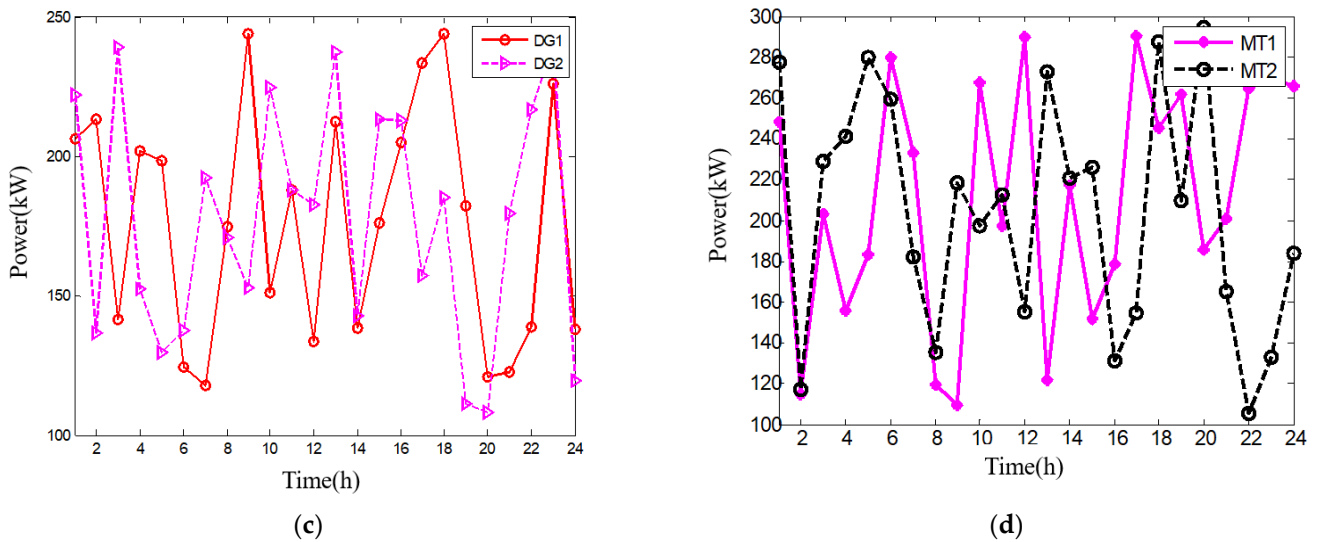


Figure 3. Operation schemes of generators and energy storage systems: (a) outputs of new energy resources; (b) outputs of energy storage units; (c) outputs of thermal power units; (d) outputs of gas turbines.

The results of power flow optimization are shown in the following figures. The *x*-axis coordinates in the figure correspond to each time of the day, and the *y*-axis coordinates correspond to the number of nodes in the system. The voltage profile in Figure 4 represents the voltage magnitude at each bus in the power system. The optimal voltage profile is kept within the acceptable range to ensure the stability and reliability of the system.

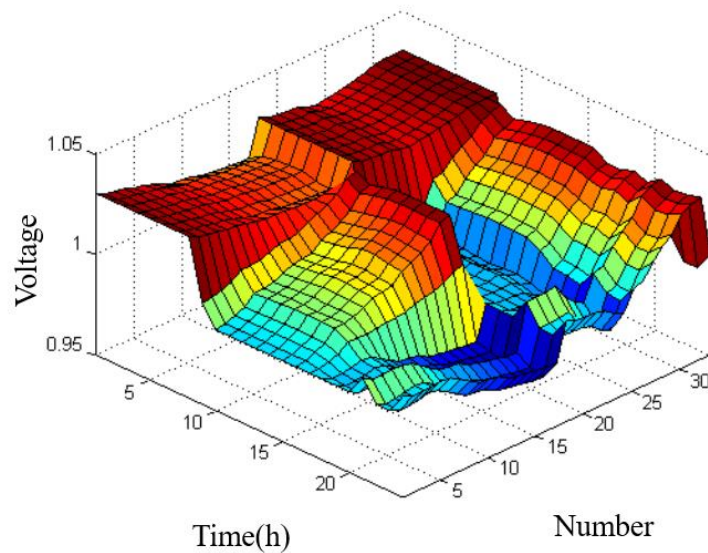


Figure 4. Voltage profile.

As depicted in Figures 5 and 6, the optimal distribution of active and reactive power flows is able to ensure efficient power transfer and voltage stability. The corresponding *z*-axis coordinates represent the per-unit values of the active power and reactive power of each node on a single-day time scale, respectively. In terms of active power flow, the optimized system exhibited a balanced distribution of power among the different transmission lines and generators, resulting in a reduction in the overloading and underutilization of some of the system components.

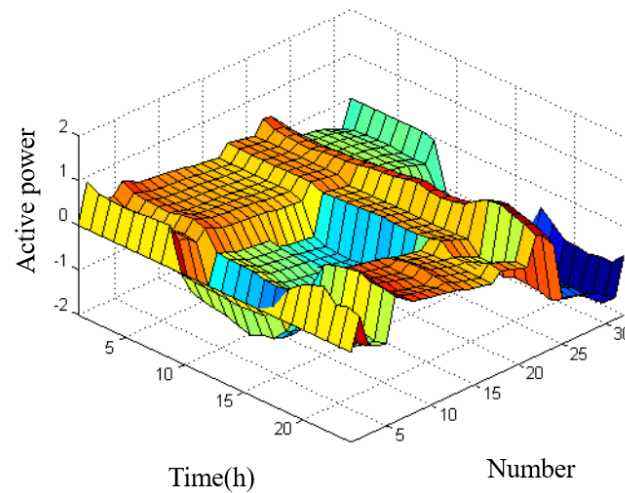


Figure 5. Active power flow.

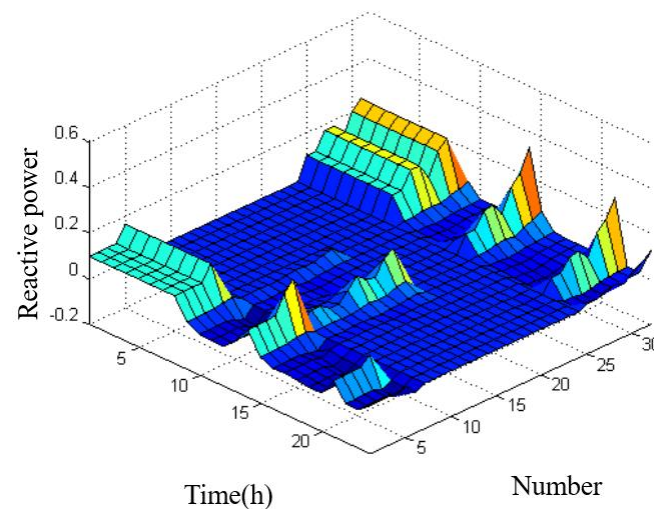


Figure 6. Reactive power flow.

These results indicate that the proposed optimization approach effectively addresses the power system transmission and generation planning problem while improving the efficiency and reliability of the system's operation. The findings can guide the design and implementation of future power system planning and operation strategies.

5. Conclusions

This paper presents a novel two-layer optimization model for generation and transmission planning that incorporates reliability and transient voltage stability considerations to tackle the challenges posed by renewable energy integration. In the transmission planning layer, the objective function is formulated by incorporating the construction cost and the EENS cost, and the constraints are designed to fully address the requirements of grid construction. In the generation and energy storage planning layer, the objective function is developed by considering the construction and operation costs and transient stability index. Moreover, the constraints of generator output, construction capacity, transient stability, system power flow, etc., are comprehensively discussed to ensure the feasibility of construction and operation. A two-layer iterative algorithm based on adaptive PSO is applied to solve the complex nonlinear problem. Case studies verify that the proposed method can effectively optimize grid planning, as well as the locations and capacities of generator sets and energy storage devices. In future studies, the impact of uncertainties such as

load demand fluctuations on the reliability and transient voltage stability of the power system planning can be further incorporated to improve the optimization effect. Through analogizing and extending the model presented in this paper, the proposed method can be implemented in actual systems.

Author Contributions: Conceptualization, F.L. and W.W.; methodology, F.L. and W.W.; software, F.L. and W.W.; validation, F.L. and W.W.; formal analysis, F.L., W.W. and D.Z.; investigation, F.L. and W.W.; resources, F.L. and W.W.; data curation, F.L., W.W. and D.W.; writing—original draft preparation, F.L. and W.W.; writing—review and editing, F.L., W.W., D.L., Z.L., X.W., H.Y. and X.S. All authors have read and agreed to the published version of the manuscript.

Funding: This research received the funding from the Science and Technology Project of State Grid Corporation of China (a study of a power grid transient stability support capability evaluation and enhancement method under the high penetration of renewable energy, 5108-202218280A-2-280-XG).

Institutional Review Board Statement: Not applicable.

Informed Consent Statement: Not applicable.

Data Availability Statement: Not applicable.

Conflicts of Interest: The authors declare no conflict of interest.

References

1. UNGA. *United Nations Framework Convention on Climate Change*; UNGA: New York, NY, USA, 1992.
2. Kang, C.; Chen, Q.; Xia, Q. Prospects of Low-Carbon Electricity. *Power Syst. Technol.* **2019**, *33*, 1–7.
3. Li, H.; Qin, B.; Jiang, Y.; Zhao, Y.; Shi, W. Data-driven optimal scheduling for underground space based integrated hydrogen energy system. *IET Renew. Power Gener.* **2022**, *16*, 2521–2531. [[CrossRef](#)]
4. Qin, B.; Sun, H.; Ma, J.; Li, W.; Ding, T.; Wang, Z.; Zomaya, A.Y. Robust H_∞ Control of Doubly Fed Wind Generator via State-Dependent Riccati Equation Technique. *IEEE Trans. Power Syst.* **2019**, *34*, 2390–2400. [[CrossRef](#)]
5. Li, J.; Li, Z.; Liu, F. Robust Coordinated Transmission and Generation Expansion Planning Considering Ramping Requirements and Construction Periods. *IEEE Trans. Power Syst.* **2018**, *33*, 268–280. [[CrossRef](#)]
6. Qin, B.; Liu, W.; Li, H.; Ding, T.; Ma, K.; Liu, T. Impact of system inherent characteristics on initial-stage short-circuit current of MMC-based MTDC transmission systems. *IEEE Trans. Power Syst.* **2022**, *37*, 3913–3922. [[CrossRef](#)]
7. Roh, J.H.; Shahidehpour, M.; Fu, Y. Market-Based Coordination of Transmission and Generation Capacity Planning. *IEEE Trans. Power Syst.* **2007**, *22*, 1406–1419. [[CrossRef](#)]
8. Tohidi, Y.; Olmos, L.; Rivier, M.; Hesamzadeh, M.R. Coordination of Generation and Transmission Development through Generation Transmission Charges—A Game Theoretical Approach. *IEEE Trans. Power Syst.* **2017**, *32*, 1103–1114. [[CrossRef](#)]
9. Qin, B.; Li, H.; Wang, Z.; Jiang, Y.; Lu, D.; Du, X.; Qian, Q. A New Framework for Low-carbon City Development of China: Underground Space Based Integrated Energy Systems. *Undergr. Space* **2023**, *early access*.
10. Moreira, A.; Pozo, D.; Street, A.; Sauma, E. Reliable Renewable Generation and Transmission Expansion Planning: Co-Optimizing System's Resources for Meeting Renewable Targets. *IEEE Trans. Power Syst.* **2017**, *32*, 3246–3257. [[CrossRef](#)]
11. Tekiner, H.; Coit, D.W.; Felder, F.A. Multi-period multi-objective electricity generation expansion planning problem with Monte-Carlo simulation. *Electr. Power Syst. Res.* **2010**, *80*, 1394–1405. [[CrossRef](#)]
12. Alizadeh, B.; Jadid, S. Reliability constrained coordination of generation and transmission expansion planning in power systems using mixed integer programming. *IET Gener. Transm. Distrib.* **2011**, *5*, 948–960. [[CrossRef](#)]
13. Baringo, L.; Baringo, A. A Stochastic Adaptive Robust Optimization Approach for the Generation and Transmission Expansion Planning. *IEEE Trans. Power Syst.* **2018**, *33*, 792–802. [[CrossRef](#)]
14. Qiu, T.; Xu, B.; Wang, Y.; Dvorkin, Y.; Kirschen, D.S. Stochastic Multistage Coplanning of Transmission Expansion and Energy Storage. *IEEE Trans. Power Syst.* **2017**, *32*, 643–651. [[CrossRef](#)]
15. Jabr, R.A. Robust Transmission Network Expansion Planning with Uncertain Renewable Generation and Loads. *IEEE Trans. Power Syst.* **2013**, *28*, 4558–4567. [[CrossRef](#)]
16. Aghaei, J.; Amjady, N.; Baharvandi, A.; Akbari, M.-A. Generation and Transmission Expansion Planning: MILP-Based Probabilistic Model. *IEEE Trans. Power Syst.* **2014**, *29*, 1592–1601. [[CrossRef](#)]
17. Zhou, Z.; He, C.; Liu, T.; Dong, X.; Dang, D.; Chen, B. Reliability-Constrained AC Power Flow-Based Co-Optimization Planning of Generation and Transmission Systems with Uncertainties. *IEEE Access* **2020**, *8*, 194218–194227. [[CrossRef](#)]
18. Choi, J. A Method for Transmission System Expansion Planning Considering Probabilistic Reliability Criteria. In Proceedings of the 2005/2006 IEEE/PES Transmission and Distribution Conference and Exhibition, Dallas, TX, USA, 21–24 May 2006; p. 1240.
19. Remon, D.; Cantarellas, A.M.; Mauricio, J.M.; Rodriguez, P. Power system stability analysis under increasing penetration of photovoltaic power plants with synchronous power controllers. *IET Renew. Power Gener.* **2017**, *11*, 733–741. [[CrossRef](#)]

20. Kabalan, M.; Singh, P.; Niebur, D. Large signal Lyapunov-based stability studies in microgrids: A review. *IEEE Trans. Smart Grid* **2017**, *8*, 2287–2295. [[CrossRef](#)]
21. Jung, J.; Cho, H.; Park, B.; Nam, S.; Hur, K.; Lee, B. Enhancement of linearity and constancy of PMU-based voltage stability index: Application to a Korean wide-area monitoring system. *IET Gener. Transm. Distrib.* **2020**, *14*, 3357–3364. [[CrossRef](#)]
22. Chowdhury, M.A.; Shen, W.; Hosseinzadeh, N.; Pota, H.R. Transient stability of power system integrated with doubly fed induction generator wind farms. *IET Renew. Power Gener.* **2015**, *9*, 184–194. [[CrossRef](#)]
23. Tajdinian, M.; Seifi, A.R.; Allahbakhshi, M. Sensitivity-based approach for real-time evaluation of transient stability of wind turbines interconnected to power grids. *IET Renew. Power Gener.* **2018**, *12*, 668–679. [[CrossRef](#)]
24. Hang, W.; Xiong, W.; Li, Z.; Song, Y. Influence of Distributed Generations on Transient Voltage Characteristics of Distribution Network. *Mod. Electr. Power* **2017**, *34*, 1–7.
25. Qin, B.; Zhang, X.; Ma, J.; Mei, S.; Hill, D.J. Local Input to State Stability Based Stability Criterion with Applications to Isolated Power Systems. *IEEE Trans. Power Syst.* **2016**, *31*, 5094–5105. [[CrossRef](#)]
26. Qin, B.; Zhang, X.; Ma, J.; Deng, S.; Mei, S.; Hill, D.J. Input-to-State Stability Based Control of Doubly Fed Wind Generator. *IEEE Trans. Power Syst.* **2018**, *33*, 2949–2961. [[CrossRef](#)]
27. Hemmati, R.; Hooshmand, R.A.; Khodabakhshian, A. Comprehensive review of generation and transmission expansion planning. *IET Gener. Transm. Distrib.* **2013**, *7*, 955–964. [[CrossRef](#)]
28. Liu, W.; Wang, Z.; Yuan, Y.; Zeng, N.; Hone, K.; Liu, X. A Novel Sigmoid-Function-Based Adaptive Weighted Particle Swarm Optimizer. *IEEE Trans. Cybern.* **2021**, *51*, 1085–1093. [[CrossRef](#)]
29. Tong, L.; Li, X.; Hu, J.; Ren, L. A PSO Optimization Scale-Transformation Stochastic-Resonance Algorithm with Stability Mutation Operator. *IEEE Access* **2017**, *6*, 1167–1176. [[CrossRef](#)]
30. Moreira, A.; Molina, Y.; Aquino, R.; Ñaupari, Z. Allocation and Sizing of Photovoltaic Systems to Reduce Power Losses and Economic Aspects using a new PSO approach. *IEEE Lat. Am. Trans.* **2022**, *20*, 977–985. [[CrossRef](#)]
31. Nguyen, T.; Morishita, H.; Koyanagi, Y.; Izui, K.; Nishiwaki, S. A Multi-Level Optimization Method Using PSO for the Optimal Design of an L-Shaped Folded Monopole Antenna Array. *IEEE Trans. Antennas Propag.* **2014**, *60*, 206–215. [[CrossRef](#)]
32. Limbu, T.R.; Saha, T.K.; McDonald, J.D.F. Value-based allocation and settlement of reserves in electricity markets. *IET Gener. Transm. Distrib.* **2011**, *5*, 489–495. [[CrossRef](#)]
33. Qin, B.; Ma, J.; Li, W.; Ding, T.; Sun, H.; Zomaya, A.Y. Decomposition-based stability analysis for isolated power systems with reduced conservativeness. *IEEE Trans. Autom. Sci. Eng.* **2020**, *17*, 1623–1632. [[CrossRef](#)]
34. Qin, B.; Wang, W.; Li, W.; Li, F.; Ding, T. Multiobjective energy management of multiple pulsed loads in shipboard integrated power systems. *IEEE Syst. J.* **2023**, *17*, 371–382. [[CrossRef](#)]
35. Santos, M.; Huo, D.; Wade, D.; Wade, N.; Greenwood, D.; Sarantakos, I. Reliability assessment of island multi-energy microgrids. *Energy Convers. Econ.* **2021**, *2*, 169–182. [[CrossRef](#)]

Disclaimer/Publisher's Note: The statements, opinions and data contained in all publications are solely those of the individual author(s) and contributor(s) and not of MDPI and/or the editor(s). MDPI and/or the editor(s) disclaim responsibility for any injury to people or property resulting from any ideas, methods, instructions or products referred to in the content.